2014 IEEE International Conference on Robotics & Automation (ICRA)
Hong Kong Convention and Exhibition Center
May 31 - June 7, 2014. Hong Kong, China

A Miniature 25 Grams Running and Jumping Robot*

Jianguo Zhao[1], Weihan Yan[1], Ning Xi[1], Matt W. Mutka[2], and Li Xiao[2]

Abstract— **In this paper, we present the design and development of a miniature robot that is able to run and jump. This robot can use wheeled locomotion to travel on the flat ground. When it encounters a large obstacle compared to its size, it can stand up and leap over the obstacle. The robot has a mass of** 25 **grams and a maximum size of** 9 **centimeters. Experimental results show that with a take-off angle** 80°**, the robot can jump up to** 1.44 **meter in height and** 0.59 **meter in distance. Moreover, it has on-board energy, control, and communication abilities, which enables tetherless or autonomous operation. With the multi-modal locomotion abilities, the robot is expected to have many applications ranging from environmental monitoring, search and rescue, to military surveillance.**

I. Introduction

Many small animals or insects with sizes less than several centimeters jump to travel in difficult environments such as bushes or forests [1]. Jumping enables them to overcome obstacles with sizes much larger than their own sizes. For example, a froghopper can jump up to 700 mm, which is more than one hundred times its size (around 6.1 mm) [2].

To mimic the jumping locomotion found in nature, we can build small robots with jumping ability. There are two major advantages for using jumping as a locomotion method. First, similar to small jumping animals or insects, small jumping robots can also overcome large obstacles relative to their sizes [3]. Second, equipped with the wireless communication ability, robots in mid-air can communicate further compared with robots on the ground [4].

Many robots with the jumping ability have been built recently. Based on their energy storage methods, they can be classified into three groups. A recent detailed review can be found in [3], and we only briefly review them here. Many robots use traditional springs to store energy. Examples include the frogbot [5], the surveillance robot [6], the Grillo [7], the EPFL jumping robot V3 [8], the CMU jumping robot [9], and our previous three generations of jumping robot [10], [11], [12]. Some robots use customized special springs as the energy storage medium. Examples include the compact jumping robot [13], the MIT microbot [14], the Jollbot [15], and the flea robot [16]. Besides the previous two energy storage mediums, there exist other methods. For example, the quadruped Airhopper [17] uses the compressed air for energy storage, while the smallest jumping microrobot is based on the microelectromechanical technology [18].

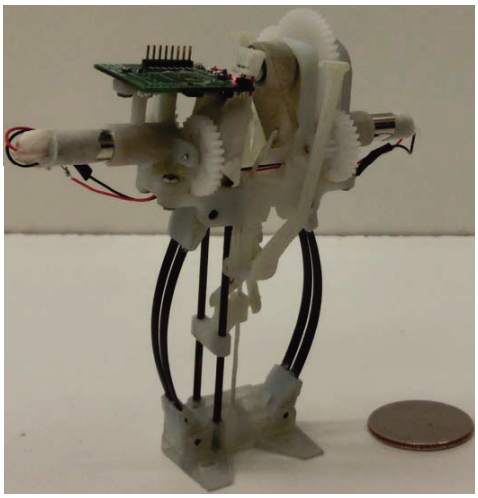

Fig. 1. Robot prototype with a US quarter on its right side.

Although jumping enables small robots to overcome obstacles, it wastes energy if robots jump in environments where no obstacle exists such as the flat ground. Therefore, it is desirable that a robot also has wheeled locomotion ability.

Researchers have also developed hybrid jumping and running robot in recent years. The scout robot used two wheels to run and a flat plate spring to directly strike the ground for jumping [19]. The Mini-Whegs employed four spoked wheels to run and a four bar mechanism driven leg to punch the ground for jumping [20]. The patrol robot utilized two wheels for running and a pneumatic driven piston to directly strike the ground for jumping [21]. The rescue robot exploited the same principle as the patrol robot [22]. The stair-climbing robot used four wheels to run and four compression springs for jumping [23]. The sand flea robot developed by Boston Dynamics, which achieved the largest jumping height to date, also had the running ability with four wheels [24].

Although all the aforementioned robots have both jumping and running ability, they target a large weight range. The lightest robot among them—the Mini-Whegs—-has a mass about 191 grams. Nevertheless, our robot is designed to be less than 30 grams. With a light weight, the robot is less susceptible to damage during the landing process. Furthermore, the robot consumes less energy for the same jumping height. Meanwhile, the lightweight requirement also presents design challenges to achieve both running and jumping.

*This research work is partially supported under U.S. Army Research Office Contract No. W911NF-11-D-0001, and U.S. Army Research Office Grant No. W911NF-09-1-0321 and W911NF-10-1-0358, and National Science Foundation Award No. CNS-1320561 and IIS-1208390.

[1]Jianguo Zhao, Weihan Yan, and Ning Xi are with Department of Electrical and Computer Engineering, Michigan State University, East Lansing, MI, 48824, USA. zhaojia1@msu.edu, yanweiha@msu.edu, xin@egr.msu.edu

[2]Matt W. Mutka and Li Xiao are with Department of Computer Science and Engineering, Michigan State University, East Lansing, MI, 48824, USA. {mutka, lxiao}@cse.msu.edu

We also designed a robot that can jump, run, and maneuver in mid-air [25]. However, that robot is mainly used to investigate the aerial maneuvering ability with an active tail. For the robot in this paper, we focus on the hybrid jumping and running locomotion. Moreover, the robot in this paper is an intensively revised and simplified design for better performances based on our previous jumping robot [3]. First, we revised the jumping mechanism using elastic strips, which simplified the design and reduced the weight. Second, we simplified the self-righting mechanism to make it more robust. Third, we revised the gear train in the energy mechanism to improve the running and turning speed. Finally, we added an embedded control system for tetherless or autonomous operations.

The main contribution of this paper is the design of a miniature robot that is able to jump and run. To the best of our knowledge, this is the first light weight robot (less than 30 grams) that has these two locomotion abilities. Moreover, the jumping performance (1.44 meter in height) of this robot is better than most of existing jumping robots as shown at the end of this paper. With such a jumping height, the robot can be used to explore other multi-modal locomotion abilities for miniature robots such as gliding or aerial maneuvering.

II. Robot Design

According to functions, we divide the robot into four parts: jumping mechanism, energy mechanism, self-righting mechanism, and running mechanism. In this section, we elaborate the design of each mechanism. Additionally, we also discuss the embedded control system for the robot.

A. Jumping Mechanism

The jumping mechanism transforms the stored energy in the robot to the kinetic energy for take-off. We use the jumping mechanism shown on the left side of Fig. 2. For this mechanism, the robot body is connected to the foot with two symmetrically placed elastic strips. The strips are connected to the body or foot with revolute joints. Two rods fixed to the foot can slide along two vertical holes in the body to make the body can only move vertically with respect to the foot. The solid model for this mechanism is shown in Fig. 6.

With the proposed jumping mechanism, a vertical downward force F applied at the top center of the body will make the body move toward the foot. In this way, the energy will be charged into the two elastic strips. Once we remove the vertical force, the stored energy will be transformed to the body's kinetic energy for take-off.

Our previous jumping mechanism uses two symmetric kinematic chains to connect the body and foot. It requires eight torsion springs to be placed at both the body and foot to store energy [3]. The revised design in Fig. 2 simplifies the design by directly using elastic strips as the energy storage medium, which eliminates both the torsion springs and the two kinematic chains.

We perform the static analysis to obtain how much force is required to compress the strips. The principle of compression belongs to the deflection of buckled slender bars. The statics

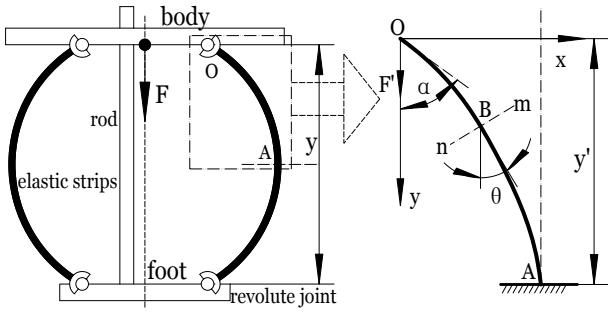

Fig. 2. Jumping mechanism and static analysis: The mechanism is shown in the left figure, where two elastic strips connect the body to the foot via four revolute joints. The static analysis for half of the right strip (OA) is shown in the right figure.

for half of one elastic strip is equivalent to the case shown on the right side of Fig. 2, where a slender bar is fixed to the ground at point A and has a free end at point O [26]. A vertical downward force F' is applied at O. We establish a coordinate system with origin at O and the axes along the directions shown in the figure.

If we consider the cross section at point B—represented by the line mn, then we have [26]

$$EI\frac{d^2\theta}{ds^2} = -F'\sin\theta \tag{1}$$

where s is the curve length from O to B, and θ is the angle between the tangent line of the bar at point B and the vertical line. Let $K = \sqrt{F'/EI}$ and α be the angle between the tangent line at point O and the vertical line. Moreover, let the total length of the strip be l, which will not change during the energy charge process, we can obtain K as [26]

$$K = \frac{1}{l}\int_0^{\pi/2} \frac{d\phi}{\sqrt{1-p^2\sin^2\phi}} \tag{2}$$

where $p = \sin\dfrac{\alpha}{2}$. Then, the force can be derived as

$$F' = K^2EI = \frac{EI}{l^2}\left(\int_0^{\pi/2} \frac{d\phi}{\sqrt{1-p^2\sin^2\phi}}\right)^2 \tag{3}$$

Given a value of α, the force can be obtained from Eq. (3). The vertical distance y' can be also derived as [26]

$$y' = \frac{1}{K}\int_0^{\frac{\pi}{2}} \frac{1-2p^2\sin^2\phi}{\sqrt{1-p^2\sin^2\phi}}d\phi \tag{4}$$

Since the model on the right side of Fig. 2 is only half of the strip in the mechanism, the required force of the jumping mechanism for a given α is $F = 2F'$, and the vertical distance between the body and foot is $y = 2y'$.

Based on the previous formulae, we obtain the force profile with respect to the vertical distance by varying the value of α from 0 to $\pi/2$. Using the force profile, we can determine the geometry of the elastic strips. Carbon fiber strips are used due to its large Young's modules and light weight. Based on the

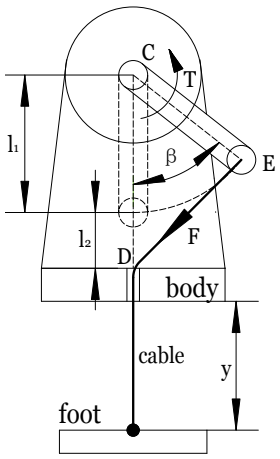

Fig. 3. Energy mechanism: the rotation link (CE) rotates counterclockwisely from the bottom to top so that the body will move towards the foot.

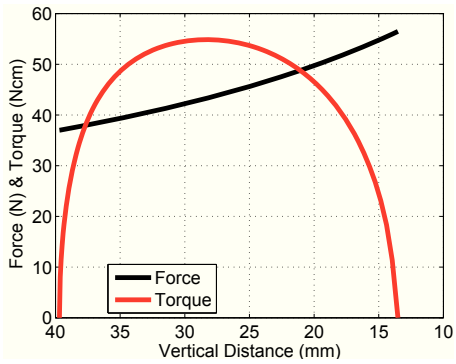

Fig. 4. The force and torque profiles during the energy charge process with the horizontal axis being the vertical distance y between the body and foot.

force profile, we choose to use the strip with a dimension of $0.4mm \times 6.0mm \times 45mm$ and a Young's Modulus of 140 GPa. The corresponding force profile with respect to the vertical distance is shown in Fig. 4.

We design the foot to have a tilt angle 10° to provide an 80° take-off angle. The reason for such an angle is that we emphasize the jumping height compared with the jumping distance due to the robot's running ability.

B. Energy Mechanism

The energy mechanism can apply and remove the force F in Fig. 2. Based on our previous design, we use a one-way bearing based gear train system [3]. As shown in Fig. 3, a rotation link CE is connected to a gear train through a one way bearing—both the gear train and the one way bearing are not shown in the figure, but they are shown in the solid model in Fig 6. A cable connects the rotation link to the foot. Therefore, if the rotation link rotates in the counterclockwise direction, then the cable will pull the foot to the body. Once the rotation link passes the vertical upward position, the energy will be released due to the one way bearing.

To design a gear train and find a corresponding motor to compress the elastic strips, we analyze the required torque to produce the desired force F shown in Fig. 2. The output torque from the gear train can be obtained from F as [3]

$$T = \frac{F l_1 (l_1 + l_2) \sin\beta}{\sqrt{l_1^2 + (l_1 + l_2)^2 - 2 l_1 (l_1 + l_2) \cos\beta}} \qquad (5)$$

where l_1 is the length of the rotation link, l_2 is the length from the end of rotation link to point D on the body, and β represents the angle that the rotation link has rotated from the initial position shown as the dashed line in Fig. 3. Both l_1 and l_2 are known from our previous jumping robot. Therefore, given a value of y—the vertical distance between body and foot, if the force F is known, we can obtain the torque T.

With the equations to compute the force and torque, we numerically plot them with respect to the vertical distance y as shown in Fig. 4. From the figure, we see that although the force increases as y decreases, the torque first increases but then decreases to zero at the end. This torque profile is good for jumping robots to prevent premature take-off [5].

To provide a sufficient torque to charge energy into the carbon fiber strips, we use a gear train to increase the output of a miniature DC motor (Part No. GH6123S from Gizmoszone). The gear train has three stages and four gears: a motor gear with 8 teeth, a compound gear with $35/8$ teeth, another compound gear with $36/9$ teeth, and a spur gear with 44 teeth. The total speed reduction ratio is thus 96.25. With a stall torque of $1.2 \times 10^{-2} Nm$ of the motor, the stall torque at the end of the gear train is $115.5 Ncm$, which is more than two times the maximum required torque obtained from the torque profile in Fig. 4.

The gear train is different from our previous design in [3]. On one hand, we change to a lighter motor. Moreover, the new motor has an output speed twice the previous one, which could increase the running speed for the running mechanism as will be discussed later. On the other hand, we increase the gear ratio to provide a sufficient output torque required for the energy charging.

C. Self-righting Mechanism

We use an active self-righting mechanism to make the robot stand up for the next jump. The robot has a rectangular shape; therefore, it will land on the ground with one of the two largest sides. As shown in Fig. 5, we place two self-righting legs on each side of the body. These two legs can rotate around revolute joints on the body. We attach a pusher to the foot, which is shown in the solid model of Fig. 6(c). During the energy charge process, the body will move towards the foot. Once the pusher contacts the two legs, it will push the two legs upward. In this way, the two legs will rotate in directions shown in Fig. 5, and the robot will stand up. Once the energy is released, the two legs will return to their original positions by two small torsion springs attached to the robot's body.

We obtain the dimension of the mechanism using the schematic shown in Fig. 5. Suppose the two legs are initially at AB and CB. After fully extended, they rotate to AB' and CB', respectively. Denote the rotation range for the left leg

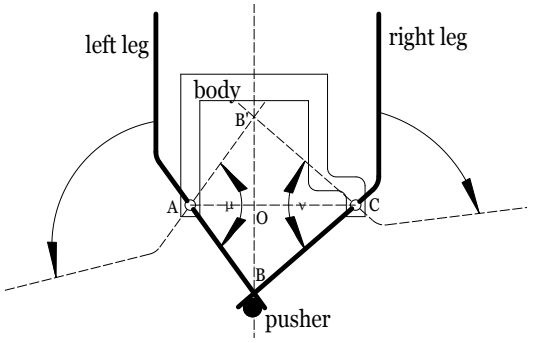

Fig. 5. Self-righting mechanism: The solid bold lines are the initial leg positions, while the dashed lines are the final positions after the self-righting.

as μ and right leg as ν. To successfully self-right from both sides, the rotation ranges for the two legs should be different due to the take-off angle being 80°. Based on our previous design, we let $\mu = 135°$ and $\nu = 115°$ to make $\mu - 10° = \nu + 10°$. Due to the size of the body, we let $AO = 5mm$ and $CO = 8mm$, then the length of each leg can be calculated as $AB = 5/\cos(135°/2) = 13.1mm$ and $CB = 8/\cos(115°/2) = 14.9mm$. The other parameters can also be obtained accordingly.

The new design is better than our previous design, which uses a tiny pin attached to the left leg to slide along a groove in the right leg [3]. First, it is simpler by getting rid of the groove structure and the pin. Second, it is more robust since the pusher directly contacts the two self-righting legs, while the old design uses a thin wall structure as the pusher to contact the tiny pin.

D. Running and Turning Mechanism

Although the jumping ability enables small robots to overcome large obstacles, jumping around in environments without obstacle wastes energy. Therefore, we equip wheeled locomotion ability to make the robot be able to roll or run on the flat ground.

The running mechanism uses four gears as wheels as shown in Fig. 6 (a) and (b). On each side of robot's body, two gears will touch the ground once the robot lands on the ground. These two gears can drive the robot to run and turn by appropriate rotating directions. One gear is actuated by the second motor, which is used solely for running. The other gear is actuated by the first motor, which is also used for jumping. Due to the one-way bearing, only one directional rotation is required for jumping and self-righting. Therefore, the other direction rotation can be used for running.

E. Embedded Control System

Besides the mechanical design, we also developed an embedded control system for wireless control or autonomous operation of the robot. The system has control, communication, and sensing abilities as is elaborated in the following.

A microcontroller ATmega128RFA1 from Atmel is used as the central processing unit. It has an integrated 2.4 GHZ RF transceiver to enable IEEE 802.15.4-compliant applications.

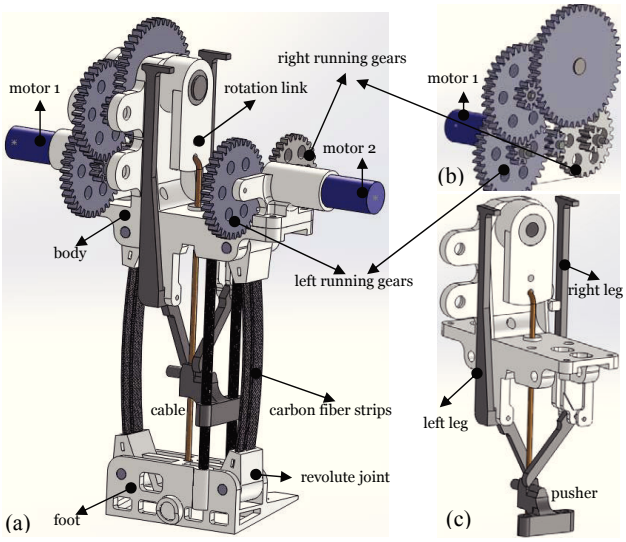

Fig. 6. Implementations of the robot: (a) The robot's solid model without the battery and the control board; (b) A detailed view of the gear train for the energy mechanism; (c) A detailed view of the self-righting mechanism.

A MPU9150 from Invensense which integrates a tri-axis gyroscope, a tri-axis accelerometer, and a tri-axis magnetometer is used for the motion sensing. With such a sensor, we can identify the robot's status to control its motion.

A MPC34933 from Freescale is used for the motor actuation. It has a dual H-bridge actuation capability, which can control the two motors' rotation directions and speeds.

An ultra low weight lithium ion battery from Powerstream with a capacity 45 mAh powers the robot. A regulator transforms the input voltage 3.7 V from the battery to 3.3 V for the system's usage.

III. Experimental Results

With the robot design discussed in the previous section, we build the robot's solid model as shown in Fig. 6(a), which includes all the mechanisms except the embedded control system and the battery. Detailed views of the self-righting mechanism and the gear train in the energy mechanism are shown in Fig. 6(c) and Fig. 6(b), respectively.

After the fabrication and assembly of the robot based on the solid model, we conducted various experiments to test the abilities of the robot. In this section, we elaborate the experimental setups and the corresponding results.

A. Jumping Experiments

We record high-speed videos to obtain the robot's jumping performance. Specifically, we place the robot in front of a white board with regular patterned holes. The distance between two neighboring holes in either horizontal or vertical direction is one inch. Then, we record the video when the robot jumps up using a high speed camera (Casio Exilim Ex-ZR400) with a frame rate 240 fps. After that, we analyze individual frames from the video to obtain the jumping performance by comparing the robot's position with the holes on the board.

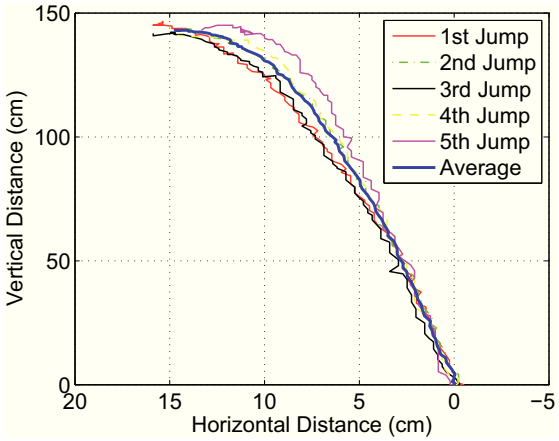

Fig. 7. Jumping experimental results: The trajectories for five jumps are shown with the robot jumping from right to left. An average trajectory is also shown for reference.

We performed five consecutive experiments, with the jumping trajectories shown in Fig. 7. Only half of each trajectory is shown due to the symmetrical property. The trajectories are obtained from the video by manually selecting the robot's position in each frame. Since the robot is not very clear in the video with high speed, it is difficult to locate the exact position in each frame. Therefore, the trajectories are not smooth as shown in the figure. In fact, the true trajectory should be a parabola if the air resistance is neglected [3].

From the five experiments, we obtain the average jumping height as 143.6 ± 2.2 cm and the average jumping distance as 59.3 ± 4.3 cm. Detailed experiments are shown in the accompanied video submission. The jumping performances are consistent since the standard deviation for five jumping is only 2.2 cm for height and 4.3 cm for distance. Compared with our previous design in [3], the robot jumps much higher because the new design reduces the foot's mass, which should be as light as possible to jump higher [3]. Furthermore, the new robot wastes less energy in mid-air since it rotates less as seen from the videos. The reason is that the new design has a smaller initial angular momentum after take-off since the motion of the body can only move linearly with respect to the foot by the two constraint carbon fiber rods.

B. Self-righting Experiments

We also conducted experiments to test the robot's self-righting ability by placing the robot on the ground. Ten experiments with a random side touching the ground are performed. The robot can stand up for all these experiments. Videos are recorded during the self-righting process. Fig. 8 shows one of the experimental results for standing up from the left side. Six frames with an equal time interval from the video are shown in the figure. An additional experiment for self-righting from the right side is included in the accompanied video submission.

Since we use two legs for self-righting, it is important to distribute the weight appropriately to make sure the robot's center of gravity lies near the two legs. Because the gear train for energy storage occupies one side of the body, we place the battery and control board on the other side of the body to balance the weight as can be seen from the robot prototype in Fig. 1.

C. Running and Turning Experiments

We tested the running and turning ability for the robot as well. The running experiment was setup as follows. We placed the robot besides a ruler, and let the robot run from left to the right and recorded the corresponding video. For the turning experiment, we placed the robot parallel to a line marker, and then let the robot turn with its maximum speed.

Experimental results are shown in the accompanied video submission. We obtain the average speed for both running and turning by analyzing the video. From the videos, both running and turning speeds vary with the surfaces on which the robot is operated. For smooth ground such as a white board shown in the video, the average running speed is 5.0 cm/s, and the average turning speed is $16^\circ/s$. For rough ground such as the cement shown in the video, the running speed decreases to 4.4 cm/s, while the turning speed surges to $150^\circ/s$.

D. Results Comparison

We compare the results with existing robots that have the running and jumping ability using the indices listed in Table I. We also include our previous jumping robot for comparison. The first index is the mass of the robot, while the second is the maximum size. The third and fourth indices list the jumping height and distance, respectively. Due to different take-off angles for each robot, we calculate the normalized jumping height with a 90° take-off angle as the fifth index using the method described in [3]. The sixth index represents the height that the robot can jump given its mass and size, which is obtained from dividing the normalized jumping height by the mass and size. The seventh index is the running speed, and the last index—similar to the sixth index—is the running speed given the robot's mass and size.

As seen in the table, the MSU Jump-runner has the lightest weight and smallest size among all the robots that have the running and jumping ability. Moreover, the jumping performance is better than all the other robots except the Sand Flea as can be seen from the normalized jumping height. If we take the mass and size into account, the MSU Jump-runner has a number 64.5, which is much larger than the Sand Flea with a number 0.37. Finally, although the running speed for MSU Jump-runner is less than the available data of Mini-Whegs and Sand Flea, it is comparable to them if we consider the mass and size as indicated by the last index in the table.

IV. Conclusions

In this paper, a miniature running and jumping robot is presented. The robot can locomote on flat ground with wheels and jump to overcome obstacles much larger than its own size. It has a compact size (9 cm) and a small mass (25 grams) including the onboard energy and control

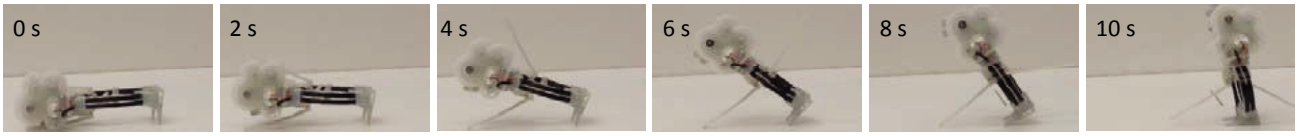

Fig. 8. Self-righting experimental results: six images extracted from a video illustrate self-righting from the left side.

TABLE I

COMPARISON WITH EXISTING ROBOTS THAT HAVE THE JUMPING AND RUNNING ABILITY

Robot Name	Mass [g]	Size [cm]	Jumping height [cm]	Jumping distance [cm]	Normalized jumping height [cm]	Height per mass and size [100·cm·/(g·cm)]	Running speed [cm/s]	Speed per mass and size [100·cm/(g·cm·s)]
Scout Robot [19]	200	11	57	×	60.6	2.75	×	×
Mini-Whegs [20]	191	10.4	18	×	19.1	0.96	90	4.5
Patrol Robot [21]	3000	25	30	0	30	0.04	×	×
Rescue Robot [22]	2300	31	80	0	80	0.11	×	×
Stair Climbing Robot [23]	3125	35	21	0	21	0.01	×	×
Sand Flea [24]	4990	45.7	800	×	850	0.37	152	0.07
MSU Jumper [3]	23.5	6.5	87.2	89.8	93.0	60.9	Not applicable	Not applicable
MSU Jump-runner	**25**	**9**	**143.6**	**59.3**	**145.1**	**64.5**	**5**	**2.2**

× Data are not available from the reference

system. Experimental results show that the robot can achieve an average jumping height 143.6 cm and a running speed of 5.0 cm/s. With such performances, the robot is an ideal platform for mobile sensing in environments with obstacles. Furthermore, the robotic platform in this paper paves the way for exploring other biologically inspired multi-modal locomotion methods such as gliding or aerial maneuvering after the robot leaps into the air.

REFERENCES

[1] R. M. Alexander, *Principles of Animal Locomotion*. Princeton University Press, 2003.

[2] M. Burrows, "Biomechanics: froghopper insects leap to new heights," *Nature*, vol. 424, no. 6948, pp. 509–509, 2003.

[3] J. Zhao, J. Xu, B. Gao, N. Xi, F. J. Cintron, M. W. Mutka, and L. Xiao, "MSU jumper: A single-motor-actuated miniature steerable jumping robot," *IEEE Trans. on Robotics*, vol. 29, no. 3, pp. 602–614, 2013.

[4] F. Cintrón, K. Pongaliur, M. W. Mutka, L. Xiao, J. Zhao, and N. Xi, "Leveraging height in a jumping sensor network to extend network coverage," *IEEE Trans. on Wireless Communications*, vol. 11, no. 5, pp. 1840–1849, 2012.

[5] J. Burdick and P. Fiorini, "Minimalist jumping robots for celestial exploration," *Int. J. Robot. Res.*, vol. 22, no. 7, pp. 653–674, 2003.

[6] J. Zhang, G. Song, Z. Li, G. Qiao, H. Sun, and A. Song, "Self-righting, steering and takeoff angle adjusting for a jumping robot," in *Proc. IEEE/RSJ Int. Conf. Intell. Robots Syst.*, Vilamoura, Algarve, Portugal, 2012, pp. 2089–2094.

[7] F. Li, W. Liu, X. Fu, G. Bonsignori, U. Scarfogliero, C. Stefanini, and P. Dario, "Jumping like an insect: Design and dynamic optimization of a jumping mini robot based on bio-mimetic inspiration," *Mechatronics*, vol. 22, no. 2, pp. 167–176, 2012.

[8] M. Kovac, M. Schlegel, J. Zufferey, and D. Floreano, "Steerable miniature jumping robot," *Auton. Robots*, vol. 28, no. 3, pp. 295–306, 2010.

[9] M. A. Woodward and M. Sitti, "Design of a miniature integrated multi-modal jumping and gliding robot," in *Proc. IEEE/RSJ Int. Conf. Intell. Robots Syst.*, San Francisco, CA, USA, 2011, pp. 556–561.

[10] J. Zhao, R. Yang, N. Xi, B. Gao, X. Fan, M. W. Mutka, and L. Xiao, "Development of a self-stabilization miniature jumping robot," in *Proc. IEEE/RSJ Int. Conf. Intell. Robots Syst.*, St. Louis, MO, USA, 2009, pp. 2217–2222.

[11] J. Zhao, N. Xi, B. Gao, M. W. Mutka, and L. Xiao, "Design and testing of a controllable miniature jumping robot," in *Proc. IEEE/RSJ Int. Conf. Intell. Robots Syst.*, Taipei, Taiwan, 2010, pp. 3346–3351.

[12] ——, "Development of a controllable and continuous jumping robot," in *Proc. IEEE Int. Conf. Robot. Autom.*, Shanghai, China, 2011, pp. 4614–4619.

[13] A. Yamada, M. Watari, H. Mochiyama, and H. Fujimoto, "A compact jumping robot utilizing snap-through buckling with bend and twist," in *Proc. IEEE/RSJ Int. Conf. Intell. Robots Syst.*, Taipei, Taiwan, 2010, pp. 389–394.

[14] S. Dubowsky, S. Kesner, J. Plante, and P. Boston, "Hopping mobility concept for search and rescue robots," *Ind. Robot*, vol. 35, no. 3, pp. 238–245, 2008.

[15] R. Armour, K. Paskins, A. Bowyer, J. Vincent, and W. Megill, "Jumping robots: a biomimetic solution to locomotion across rough terrain," *Bioinsp. Biomim.*, vol. 2, no. 3, pp. 65–82, 2007.

[16] M. Noh, S.-W. Kim, S. An, J.-S. Koh, and K.-J. Cho, "Flea-inspired catapult mechanism for miniature jumping robots," *IEEE Trans. on Robotics*, vol. 28, no. 5, pp. 1007–1018, 2012.

[17] T. Tanaka and S. Hirose, "Development of leg-wheel hybrid quadruped airhopper: Design of powerful light-weight leg with wheel," in *Proc. IEEE Int. Conf. Robot. Autom.*, Pasadena, CA, USA, 2008, pp. 3890–3895.

[18] W. Churaman, A. P. Gerratt, and S. Bergbreiter, "First leaps toward jumping microrobots," in *Proc. IEEE/RSJ Int. Conf. Intell. Robots Syst.*, San Francisco, CA, USA, 2011, pp. 1680–1686.

[19] S. A. Stoeter and N. Papanikolopoulos, "Kinematic motion model for jumping scout robots," *IEEE Trans. Robot. Autom.*, vol. 22, no. 2, pp. 398–403, 2006.

[20] B. G. A. Lambrecht, A. D. Horchler, and R. D. Quinn, "A small, insect inspired robot that runs and jumps," in *Proc. IEEE Int. Conf. Robot. Autom.*, Barcelona, Spain, 2005, pp. 1240–1245.

[21] D. H. Kim, J. H. Lee, I. Kim, S. H. Noh, and S. K. Oho, "Mechanism, control, and visual management of a jumping robot," *Mechatronics*, vol. 18, no. 10, pp. 591–600, 2008.

[22] E. Watari, H. Tsukagoshi, A. Kitagawa, and T. Tanaka, "A higher casting and jump motions realized by robots using magnetic brake cylinder," *ASME J. Mech. Robot.*, vol. 3, no. 4, 2011.

[23] K. Kikuchi, K. Sakaguchi, T. Sudo, N. Bushida, Y. Chiba, and Y. Asai, "A study on a wheel-based stair-climbing robot with a hopping mechanism," *Mech. Syst. Sig. Pr.*, vol. 22, no. 6, pp. 1316–1326, 2008.

[24] E. Ackerman, "Boston dynamics sand flea robot demonstrates astonishing jumping skills," IEEE Spectrum Robotics Blog, 2012.

[25] J. Zhao, T. Zhao, N. Xi, F. J. Cintron, M. W. Mutka, and L. Xiao, "Controlling aerial maneuvering of a miniature jumping robot using its tail," in *Proc. IEEE/RSJ Int. Conf. Intell. Robots Syst.*, Tokyo, Japan, 2013, pp. 3802–3807.

[26] S. Timoshenko, *Theory of Elastic Stability*. McGraw-Hill Book Company, Inc, 1936.